INFECTION AND IMMUNITY, Aug. 2011, p. 3291–3301 Vol. 79, No. 8
0019-9567/11/$12.00 doi:10.1128/IAI.00200-11

In Vivo Ultrastructural Analysis of the Intimate Relationship between Polymorphonuclear Leukocytes and the Chlamydial Developmental Cycle▽

Roger G. Rank,[1]* Judy Whittimore,[2] Anne K. Bowlin,[1] and Priscilla B. Wyrick[2]

Departments of Microbiology and Immunology, University of Arkansas for Medical Sciences and Arkansas Children's Hospital Research Institute, Little Rock, Arkansas,[1] and Department of Microbiology, J. H. Quillen College of Medicine, East Tennessee State University, Johnson City, Tennessee[2]

Received 25 February 2011/Returned for modification 11 April 2011/Accepted 6 May 2011

We utilized a recently developed model of intracervical infection with *Chlamydia muridarum* in the mouse to elicit a relatively synchronous infection during the initial developmental cycle in order to examine at the ultrastructural level the development of both the chlamydial inclusion and the onset of the inflammatory response. At 18 h after infection, only a few elementary bodies attached to cells were visible, as were an occasional intracellular intermediate body and reticulate body. By 24 h, inclusions had 2 to 5 reticulate bodies and were beginning to fuse. A few polymorphonuclear leukocytes (PMNs) were already present in the epithelium in the vicinity of and directly adjacent to infected cells. By 30 h, the inclusions were larger and consisted solely of reticulate bodies, but by 36 to 42 h, they contained intermediate bodies and elementary bodies as well. Many PMNs were adjacent to or actually inside infected cells. Chlamydiae appeared to exit the cell either (i) through disintegration of the inclusion membrane and rupture of the cell, (ii) by dislodgement of the cell from the epithelium by PMNs, or (iii) by direct invasion of the infected cell by the PMNs. When PMNs were depleted, the number of released elementary bodies was significantly greater as determined both visually and by culture. Interestingly, depletion of PMNs revealed the presence of inclusions containing aberrant reticulate bodies, reminiscent of effects seen *in vitro* when chlamydiae are incubated with gamma interferon. *In vivo* evidence for the contact-dependent development hypothesis, a potential mechanism for triggering the conversion of reticulate bodies to elementary bodies, and for translocation of lipid droplets into the inclusion is also presented.

Perhaps one of the most interesting and unique aspects of chlamydiae is their two-stage developmental cycle. That chlamydiae have a biphasic cycle was first described by Bedson and Bland (3) in 1932, and since that time, there have been a tremendous number of papers devoted to the description of the morphology and the regulation of the developmental cycle. The morphology of chlamydiae at the ultrastructural level has been repeatedly presented using a variety of ultrastructural techniques, such that we have a very extensive picture of reticulate bodies (RBs) and elementary bodies (EBs) both in cross-section by transmission electron microscopy (TEM) and of the surface by scanning and freeze fracture (12). Moreover, there are also an extensive number of photographs available of the organism residing intracellularly in many different cell types. While the vast majority of ultrastructural pictures of chlamydiae are derived from *in vitro* culture, there have been fewer reports, although still a significant number, showing chlamydiae *in vivo* (17, 18, 25, 26). All of these reports have allowed us to deduce the sequence of events in the developmental cycle.

Nevertheless, despite this large source of morphological information, there is still very limited information on the course of the developmental cycle in a living animal. The pictures available from *in vivo* preparations are from but a snapshot in time, virtually all being from several days or more following infection. To a great extent, this is because chlamydial infections are asynchronous, such that one finds multiple stages of inclusions at a given time in the presence of the inflammatory response. While one can glean knowledge of the events that are occurring during the cycle, it has been impossible to accurately characterize the events that occur from the initial infection of cells in an epithelium through to the exit of EBs from the cells. With regard to that particular point, we do not know what the actual exit strategy is for chlamydiae *in vivo*. There are a number of different theories based on *in vitro* studies (4, 8, 15, 30), but whether these bear any resemblance to reality or are strictly artifacts of the *in vitro* culture is unknown.

Furthermore, it is patently obvious that there is an intense innate host response associated with *in vivo* infection, initially predominated by polymorphonuclear leukocytes (PMNs). What is the impact of this response on the chlamydial developmental cycle? In a recent paper, we examined guinea pig conjunctivas infected with *Chlamydia caviae* at the ultrastructural level (22). Interestingly, we observed that PMNs appeared to actually be "pushing" the infected cells off the epithelium even before the inclusions were mature. We suggested that PMNs play a role in dissemination of chlamydiae that may actually be beneficial to the survival of the organism. We also found evidence for PMN-mediated cell destruction as well as phagocytosis of chlamydial EBs and RBs. Thus, it is clear that PMNs are intimately associated with the chlamydial developmental cycle in regard to beneficial and harmful effects for the organism as well as the host.

In the present study, we took advantage of a recently developed model of intracervical infection in the mouse in which a relatively synchronous infection can be elicited during the pri-

* Corresponding author. Mailing address: Arkansas Children's Hospital Research Institute, 13 Children's Way, Little Rock, AR 72202. Phone: (501) 364-2474. Fax: (501) 364-2403. E-mail: rankrogerg@uams.edu.

▽ Published ahead of print on 16 May 2011.

mary developmental cycle to examine at the ultrastructural level the sequential development of both the chlamydial inclusion and the onset of the inflammatory response (21). Using this model, we have been able to characterize stepwise at 6 h intervals the *in vivo* developmental cycle, including the mechanisms by which the chlamydiae exit their host cell. Furthermore, by depleting PMNs, we are able to demonstrate *in vivo* inclusions containing aberrant reticulate bodies identical to those induced by gamma interferon (IFN-γ) *in vitro*.

MATERIALS AND METHODS

Experimental animals. Six-week-old C57BL/6 mice were obtained from Jackson Laboratories (Bar Harbor, ME) and were housed in a barrier facility with a 12 h-12 h light-dark cycle and food and water *ad libitum*.

Intracervical inoculation of chlamydiae and quantification of infection. The Nigg strain of *Chlamydia muridarum* was utilized in these experiments. The culture was originally obtained from ATCC as a yolk sac preparation in 1977 and has been subsequently passaged in this laboratory, first in yolk sacs and then in cell culture. Seven days prior to infection, mice were injected subcutaneously with 25 mg (each) of medroxyprogesterone (Depo-Provera) to force the mice into a state of anestrus, thus ensuring that all mice were inoculated at the same stage of the estrous cycle to eliminate that variable. The number of inclusion-forming units (IFU) in cervicovaginal swabs and in cervical tissue from mice was determined by culturing in McCoy cells according to standard protocols (20).

On the day of infection, mice were anesthetized with 5 mg/kg of pentobarbital (Nembutal) intraperitoneally. The lower abdomen was shaved and swabbed with Betadine and 70% ethanol. A 1-cm incision was made ventrally in the skin followed by blunt dissection of the peritoneum directly over the cervix. The uterine horns were exposed, and the left horn was ligated directly distal of the uterine horn branching point using a medium LigaClip (Ethicon Endo-Surgery, Inc., Cincinnati, OH). The right horn was ligated approximately 1 cm distal of the branching point. The chlamydial inoculum containing 10^7 IFU in 20 μl of sucrose-phosphate-glutamate buffer (SPG), pH 7.2, was injected into the right uterine horn immediately proximal to the ligation point in the direction of the endocervix using an insulin syringe fitted with a 30-g, 0.5-inch needle bent at a 45° angle. The skin was then closed with a standard surgical staple. This method permitted the deposition and containment of the chlamydial suspension directly at the endocervix, which is the primary target tissue of chlamydial genital infection. Moreover, the site of injection in the uterine horn was designed to preclude any damage to the endocervix itself by mechanical insertion of the needle. A large number of IFU was used so that a high infection rate could be obtained to facilitate detection and observation of chlamydiae and infected cells by TEM. All animal experiments were preapproved by the Institutional Animal Care and Use Committee of the University of Arkansas for Medical Sciences.

Depletion of PMNs. In order to deplete PMNs, mice were injected intraperitoneally with 100 μg (each) of antibody specific for mouse PMNs (rat anti-mouse Ly-6G/Ly-6C [Gr-1]; BioLegend, San Diego, CA) 24 h prior to intracervical infection, at the time of infection, and 24 h after infection. Control mice were injected similarly with a rat IgG2b isotype control (BioLegend). At 42 and 48 h after intracervical infection with 10^7 IFU, cervicovaginal swabs were collected and placed in 2-sucrose-phosphate (2-SP) transport medium (29). The mice were then euthanized, the cervices were removed and placed in transport medium, and the number of IFU was determined by culture in McCoy cells.

Electron microscopy. Following euthanasia, the cervix of the mouse was dissected free of the vagina and uterine horns, and a gel-loading tip (catalog number 05-408-151; Fisher) with approximately 0.5 cm of the tip removed was inserted gently through the cervical os. The cervix was then separated from the uterine horns at the level of the bifurcation of the uterus. The cervix, including the gel-loading tip, was placed in 2% glutaraldehyde-0.5% paraformaldehyde, in 0.1 M Cacodylate buffer (pH 7.2), for subsequent standard processing, infiltration, and embedding in Epon 812 resin for high-contrast TEM (31). Sequential semithin sections of sagittal views of the cervical tissue were cut, placed on a glass side, stained with epoxy tissue stain (EM Sciences, Hatfield, PA), which is a toluidine blue O/basic fuchsin in a water/alcohol solution, and examined by bright-field microscopy for orientation. When the section depth revealed areas of early inflammation, indicating the likely presence of chlamydial infection, the area was isolated and retrimmed, and silver-gold thin sections were cut with a diamond knife using a Leica Ultracut S ultramicrotome (Leica Microsystems, Inc., Bannockburn, IL), collected on copper grids, and examined with a Philips Tecnai-10 electron microscope (FEI) at 80 kV.

For evaluation of the TEMs, multiple thin sections of one level were obtained after localization by obtaining a thick section, and approximately 20 to 30 photographs per thin slice were observed. Next, another thick section was obtained, and again, as many as 20 to 30 photographs per thin slice were observed. This was repeated at least one more time, so that ultimately, multiple thin sections were examined at three different depths of the tissue. Moreover, an even larger amount of tissue was examined under the microscope before pictures were taken. This procedure ensured that a large amount of tissue was examined. Therefore, photographs presented in this paper are not isolated observations but are representative of many observations of the reported phenomenon.

Determination of bacterial area. The area of RBs was determined using Image J software (NIH). Individual RBs were outlined, and the area was calculated. The data were entered into an Excel spreadsheet, and means and medians were determined. In order to determine the area of the inclusion membrane-attached RBs versus that of RBs that were not attached, we utilized electron photomicrographs at 36 h after infection, when there were sufficient numbers of visible RBs attached and unattached to perform optimal statistical analysis. Only those RBs that were obviously in contact with the inclusion membrane were considered to be membrane attached. Other RBs in close proximity to but not attached to the inclusion membrane may have been attached at a different level, but since this could not be verified, they were counted as unattached.

Experimental design. Because we were interested only in the host response to chlamydiae within the time span of the first developmental cycle, the cervix was collected from a single mouse at 18, 24, 30, 36, 42, and 48 h following intracervical inoculation. This enabled us to characterize the developmental cycle and the inflammatory response as it developed immediately following infection. We had previously noted that PMNs began to appear in the submucosa of the endocervix approximately 12 h after infection but had not yet reached the epithelium (10). In the experiments in which PMNs were depleted, cervical tissue for TEM was collected at 36 and 42 h based on our observations in intact mice. For quantification of chlamydiae, cervical tissues were collected at 42 and 48 h after infection.

RESULTS

Stepwise examination of the *in vivo* chlamydial developmental cycle. While previous *in vitro* studies suggested that chlamydial replication began to occur as early as 12 h after infection, examination of endocervical tissue at 18 h by TEM still demonstrated only single EBs, either intraluminal or attached to the cell surface, and/or single intermediate bodies (IBs) or single RBs. In Fig. 1A, a single IB is seen just within the host cell plasma membrane. An occasional RB was also seen at 18 h after infection (Fig. 1B). It was somewhat surprising that only single organisms were present by 18 h after infection, but one must consider that there is a mucous layer *in vivo* that may impede or at least slow down attachment of the organism to the target cells.

However, by 24 h after infection, it was obvious that chlamydial replication was well under way. Multiple inclusions containing 1 to 5 RBs were observed (Fig. 2A and B), although since the TEMs represent a single ultrathin slice, the inclusions undoubtedly contain more RBs. It was interesting that many inclusions within a single cell were observed, but just 6 h later in infection, only a single inclusion for a given host cell was observed. These observations strongly indicate that fusion of the inclusions occurs between 24 and 30 h following infection *in vivo*. In fact, evidence suggesting fusion of inclusions can be seen in Fig. 2A. Even though all of the inclusions contained only a few RBs, PMNs and an occasional NK-like cell could already be found in the epithelium, generally in the proximity of infected cells (Fig. 2C and D). In fact, it was common to find PMNs in actual contact with infected cells, even when the cells had only a single RB in the inclusion (Fig. 2C and D). This clearly indicated that a strong chemokine gradient, sufficient to allow PMNs to discriminate between infected and uninfected

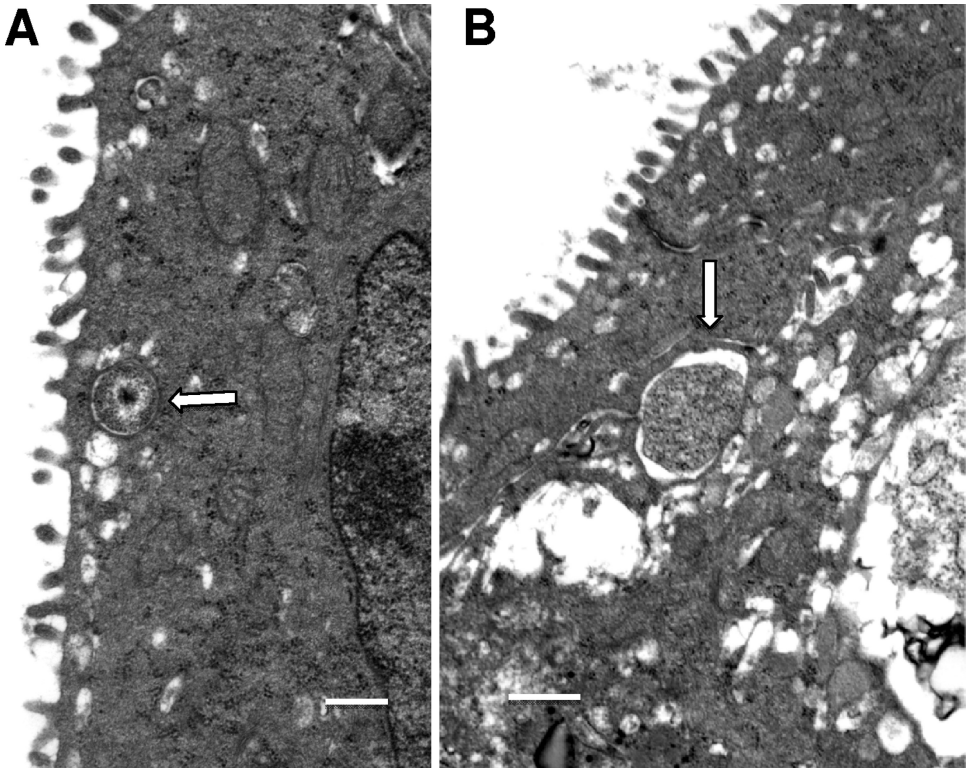

FIG. 1. Initial stages of chlamydial infection at 18 h after mouse endocervical inoculation. (A) Note an intermediate body (arrow) within an endosomal vacuole. (B) Inclusion with a single RB (arrow). Scale bars: 500 nm.

cells, had already been produced by the infected cell(s). In contrast to PMNs that were present in the epithelium somewhat distant from infected cells, those PMNs actually abutting infected cells often had prominent pseudopodia in contact with the cell or making an indentation into the cell membrane (Fig. 2C). This clearly suggested a "targeting" of the infected cell by the PMN and recognition that the target cell was infected. This phenomenon was not observed with PMNs adjacent to uninfected cells. At this point in the infection, with the exception of the presence of PMNs, the epithelium appeared quite healthy, and even the infected cells did not appear damaged in any way.

By 30 h after infection, the inclusions had increased in size and contained actively dividing RBs (Fig. 3A). Cells contained only single inclusions, so it was apparent that the fusion process had been completed by this time. PMNs were in evidence in the vicinity of infected cells as observed at 24 h. The tissue epithelium was still intact without evidence of significant tissue destruction.

However, by 36 h after infection, a variety of important events began to occur. Inclusions were larger, and conversion of RBs to EBs was under way. Many RBs were still observed, but IBs and EBs were more plentiful (Fig. 3B and D). At this time, one could begin to see evidence of three different mechanisms by which inclusions were terminated and how chlamydiae may be released at the end of the developmental cycle. Again, as seen at 24 and 30 h, PMNs were adjacent to and in contact with infected cells (Fig. 3B to D). In some cases, it appeared that the PMNs were dislodging the intact infected cells from the epithelium as we have described previously for *C. caviae*-infected conjunctivas in guinea pigs (Fig. 3C and D) (22). Thus, it is likely that the infected cell would break apart in the lumen and distribute free EBs. In some cases, the inclusion was apparently disintegrating within the host cell, i.e., the inclusion membrane was no longer present, and the chlamydiae were free in the cytoplasm (Fig. 3C). In such cases, the host cell itself was not healthy.

Perhaps the most exciting observation was that in several instances, PMNs had clearly penetrated into the infected host cell cytoplasm and were in direct contact with the inclusion (Fig. 4A to C). This scenario was observed at 48 h, when an infected cell was observed with an intracellular PMN directly in contact with chlamydiae after the inclusion membrane had broken down (Fig. 4C). One can very easily observe small pseudopodia in direct contact with chlamydiae. In the particular case shown in Fig. 4C, the host cell is clearly severely damaged, as evidenced by the lack of microvilli, and it is being released from the epithelium. An alternative mechanism by which the PMNs may complete the destruction of the host cell is shown in Fig. 4D, in which the host cell has lysed, leaving only cellular fragments and many chlamydiae present. A PMN, which may have been inside in the cell, can be observed, suggesting that the PMN destroyed the infected host cell from within.

It is quite apparent that the initial *in vivo* developmental cycle is complete within 42 to 48 h after inoculation. At 48 h, there were large intact inclusions with many EBs but also a large number of infected cells with inclusions in which the inclusion membrane was no longer present, so that there were

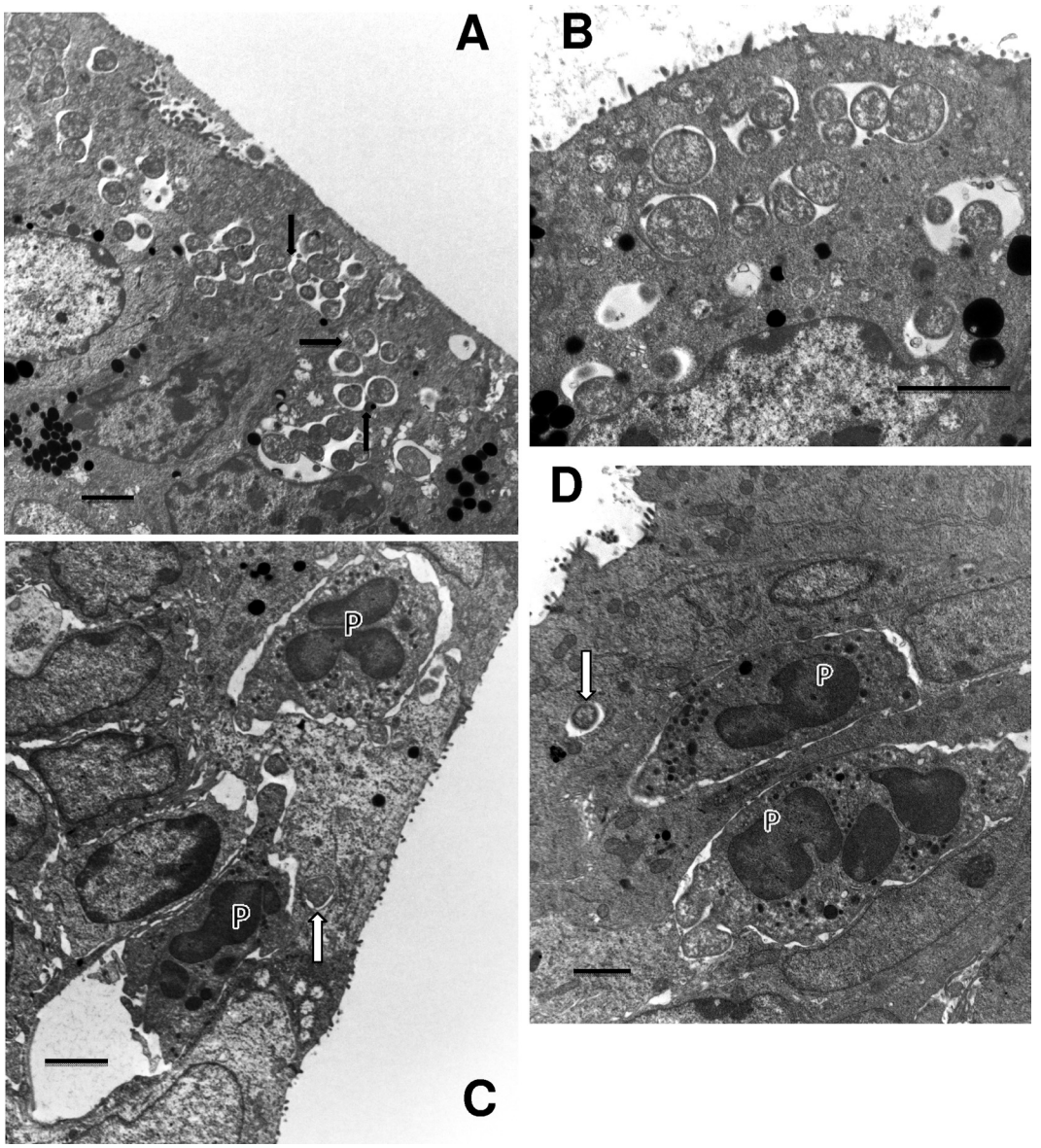

FIG. 2. Events occurring 24 h after infection. (A) Multiple early inclusions containing one to a few RBs. Some epithelial cells contain multiple inclusions. RBs are clearly dividing, and the proximity of inclusions suggests that the fusion process is under way (arrows). (B) Enlarged view of early, 24-h inclusions clearly showing multiple inclusions in a single cell. The RBs are generally larger at this time of the cycle in preparation for division than at later times. (C) PMNs (P) are seen directly in contact with an infected cell even though only a single RB (arrow) is present. Note the obvious pseudopodia of the PMNs extending toward and actually forming pockets in the infected cell. (D) Another view showing PMNs (P) in contact with an infected cell containing a single RB (arrow). Scale bars: 2 μm.

RBs and many EBs present directly in the cytoplasm (Fig. 5A to C). In some cases, PMNs were adjacent (Fig. 5B), but it appeared that by this time in the cycle, the host cell was not able to sustain the inclusion. While PMNs could facilitate the dislodgement of infected cells from the epithelium (Fig. 3B), in other cases (Fig. 5C), the infected cells became dislodged in a mechanism probably similar to that by which dead or dying cells are normally deleted from the epithelium. Interestingly, of all of the many infected cells that were viewed, there was no obvious morphological evidence of apoptosis of the infected cells.

Another phenomenon observed in an *in vitro* study is the translocation of lipid droplets into the inclusion (5). It was not uncommon to observe lipid droplets in infected cells, some of which were directly associated with the inclusion, and others that were entering into the inclusion (Fig. 6B), supporting the *in vitro* observations.

Contact-dependent development. One of the important questions regarding the developmental cycle is that of the events or signals that initiate the transition of an RB to an EB. One theory put forth by Wilson and colleagues is the contact-dependent hypothesis of chlamydial development, in which RBs can replicate and develop only when in contact with the inclusion membrane via type III secretion injectisomes; when type III secretion is disrupted through detachment or another

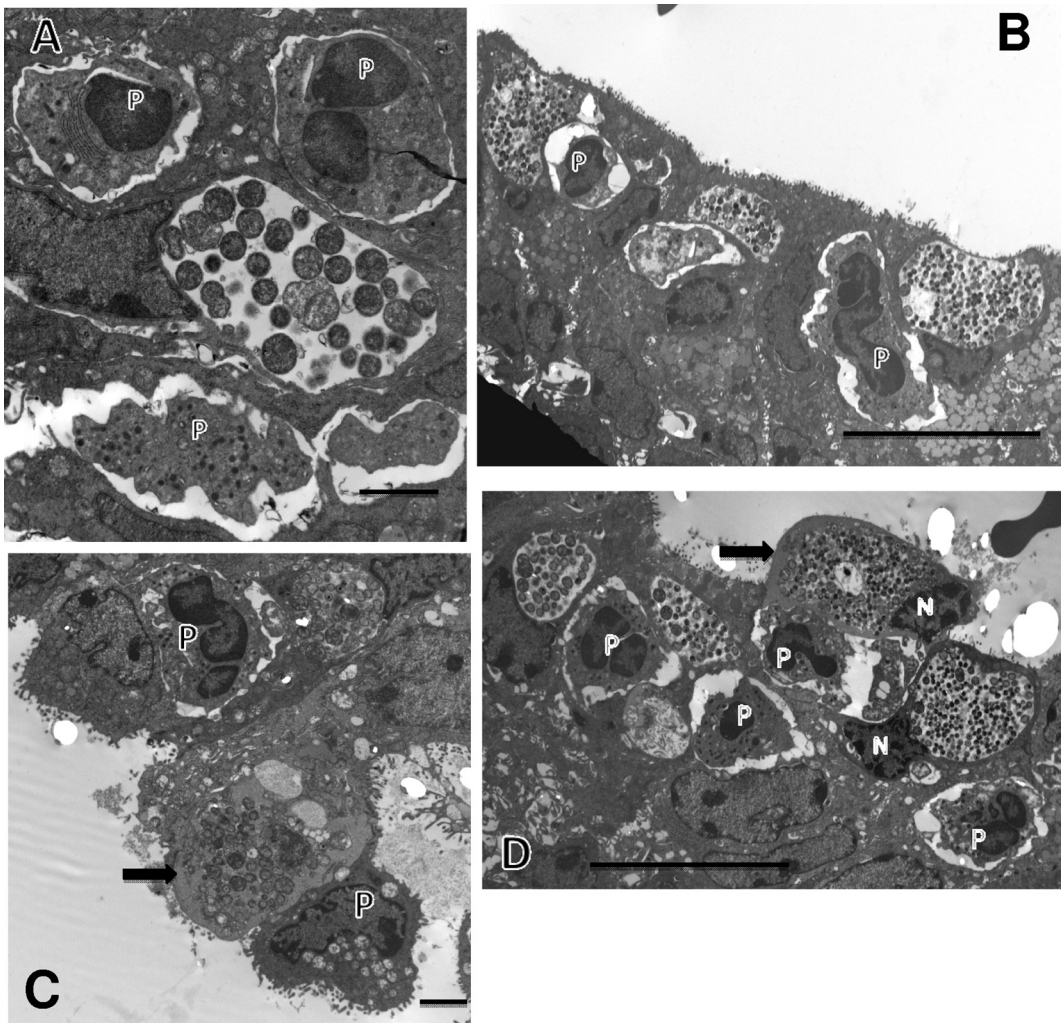

FIG. 3. Events at 30 and 36 h after infection. (A) Inclusion with multiple RBs at 30 h after infection and PMNs (P) in contact with the infected epithelial host cell. (B) By 36 h after infection, the inclusions have increased dramatically in size and contain plentiful EBs, indicating that the inclusion is in its late stages. PMNs (P), again, abut the infected epithelia. (C) An infected cell, with PMNs (P) on either side (arrow), is becoming detached from the epithelium. Note that the inclusion membrane is no longer apparent and the chlamydiae appear to be free in the cytoplasm. The highly vacuolated nature and lack of microvilli of the infected cell suggest that the epithelial cell is dying. (D) Multiple large mature inclusions are seen. In particular, one infected cell (arrow) is being detached from the epithelium with a PMN (P) directly in the space beneath the cell, giving the appearance of "pushing" the cell off the epithelial surface; the PMN appears to have phagocytized numerous RBs. Nuclei (N) of the infected cells are visible. Scale bars: 2 μm (A and C), 10 μm (B and D).

mechanism, RBs then begin the transition to EBs (28). As observed in the present study, especially late in the developmental cycle, at about 42 to 48 h, there were many inclusions for which the majority of the RBs in the inclusion were associated with the inclusion membrane while EBs and IBs were in the interior of the inclusion (Fig. 6A and B). By visual examination, it appeared that RBs that were not attached to the inclusion membrane were smaller than those that were attached. Also, as the developmental cycle progressed, the RBs in general appeared to be smaller in area.

To verify these observations, the area of all RBs in multiple micrographs at 24, 30, and 36 h after inoculation was determined using Image J software. As recorded in Table 1, the area of individual RBs decreased dramatically from 24 to 30 and 36 h. The difference in RB area between 30 h and 24 h was significantly decreased (P was <0.001 by a one-way analysis of variance [ANOVA] with Tukey *post hoc* analysis), and the difference in RB area between 36 and 30 h as well as 24 h was also significant, with a P value of <0.001. Furthermore, the areas of membrane-attached and unattached RBs at 36 h after infection were measured. The unattached RBs were significantly decreased in area compared to the areas of attached RBs ($P < 0.003$). This is consistent with the contact-dependent hypothesis of chlamydial development, whereby the area of contact between an RB and the inclusion membrane is gradually reduced (Fig. 7A and B).

Contribution of PMNs to clearance of chlamydiae. While it would seem intuitive that PMNs are critical for the control of chlamydial infection, even in the initial developmental cycle, we wanted to determine the impact of PMNs within the first 48 h of infection. PMNs were depleted from six mice by treatment with rat anti-mouse Ly-6G/Ly-6C, while six control mice

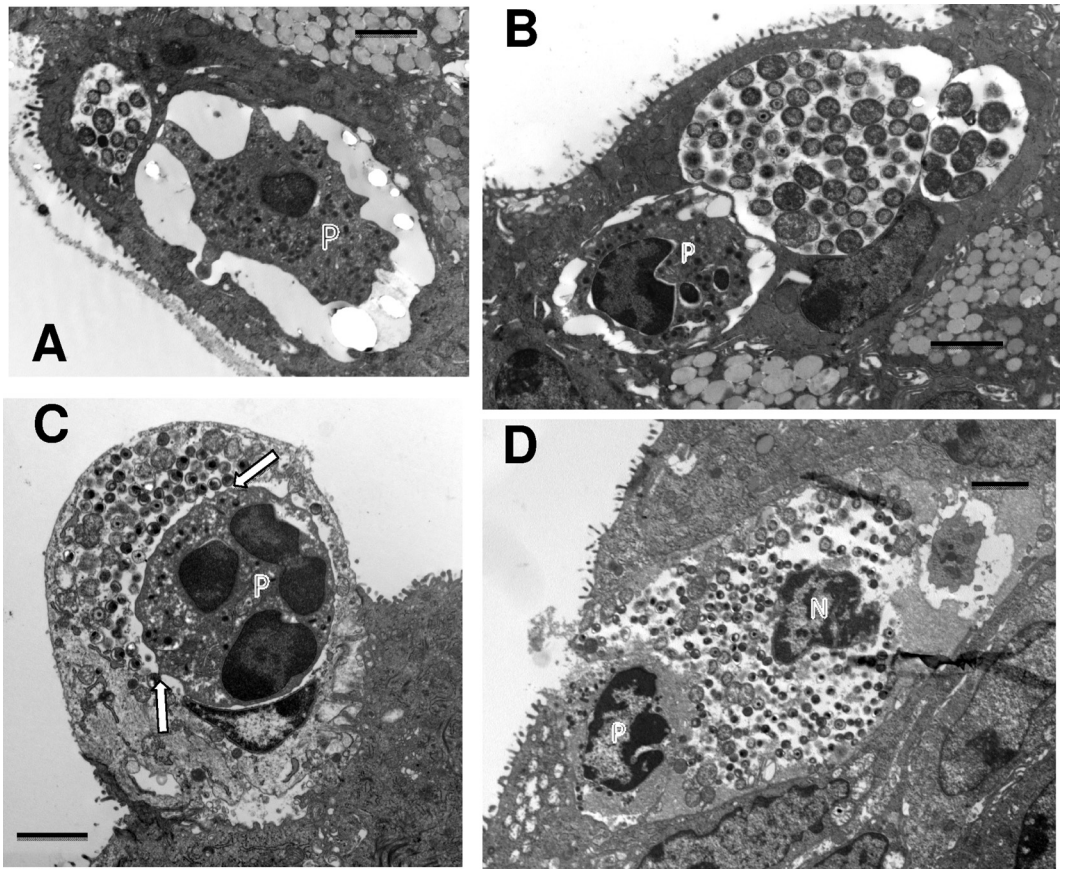

FIG. 4. PMNs enter into the infected host epithelial cell to make direct contact with chlamydiae. (A) At 42 h after infection, a PMN has gained access to and is completely inside the infected target cell. Note the extended pseudopodia, one directly in contact with the epithelial cell cytoplasm close to the inclusion. (B) Another view showing an invading intracellular PMN directly in contact with the chlamydial inclusion membrane. (C) The inclusion membrane is no longer apparent, and the intracellular PMN is in direct contact with chlamydiae. Note the projections from the PMNs touching the IBs or EBs (arrows). (D) A PMN (P) within a large space containing chlamydiae and cellular debris, including a cell nucleus (N), suggesting either that this epithelial cell was destroyed by the action of the PMN or that the PMN has entered the site following lysis of the cell. Scale bars: 2 μm (A and C), 10 μm (B and D).

were treated with an irrelevant isotype control antibody. At 42 and 48 h after intracervical infection, cervicovaginal swabs were collected, cervices were removed, and the number of IFU was determined. When the IFU obtained at each time were quantified, there was no increase in IFU in the control animals between 42 and 48 h in either swabs or tissue (Fig. 8). However, in the PMN-depleted mice, there was a significant increase in the number of IFU between 42 and 48 h in both swabs ($P < 0.005$) and tissue ($P < 0.02$), according to a one-tailed t test. These data strongly indicated that PMNs, even within the time frame of the first developmental cycle, play an important role in controlling the infection.

To determine what impact depletion of PMNs had at the ultrastructural level, cervical tissue was collected from a PMN-depleted mouse at 42 and 48 h postinfection and processed for electron microscopy; the images were compared to those of normal mice at the equivalent times. The depleted tissue, as expected, showed a paucity of PMNs. An occasional PMN was observed, but it was a rare occurrence compared to those seen in immunologically normal mice, indicating that the antibody treatment was successful in depleting the vast majority of PMNs. In general, the inclusions in the PMN-depleted cervices were larger at both 42 and 48 h than those in control mice. By 42 to 48 h, there were large numbers of EBs in the lumen and even evidence of a second round of infection that was not seen in the control cervix. The primary mechanism of EB release appeared to be the breakdown of the inclusion membrane and *in situ* lysing of the infected cell, as seen in Fig. 6A and C.

Surprisingly, in the cervix of the PMN-depleted animal at 48 h after inoculation, inclusions containing aberrant RBs were observed (Fig. 9A to C). These inclusions were completely reminiscent of those seen in culture with IFN-γ or penicillin. The aberrant RBs were significantly larger than RBs seen in normal inclusions at 42 h, with an average area of 0.87 ± 0.29 μm compared to 0.31 ± 0.16 μm^2 for normal RBs (P value, <0.00001 according to a one-tailed t test). Groups of miniature RBs were also commonly observed adjacent to the aberrant RBs, again analogous to observations of RB morphologies in IFN-γ-exposed tissue culture. In addition, the inclusions with aberrant RBs were essentially devoid of glycogen, which was readily apparent in normal inclusions (Fig. 9A and B). Interestingly, lipid droplets could be seen entering the inclusions with aberrant RBs, much as that seen in normal inclusions (Fig. 9A). Occasionally, we also noted inclusions that had both

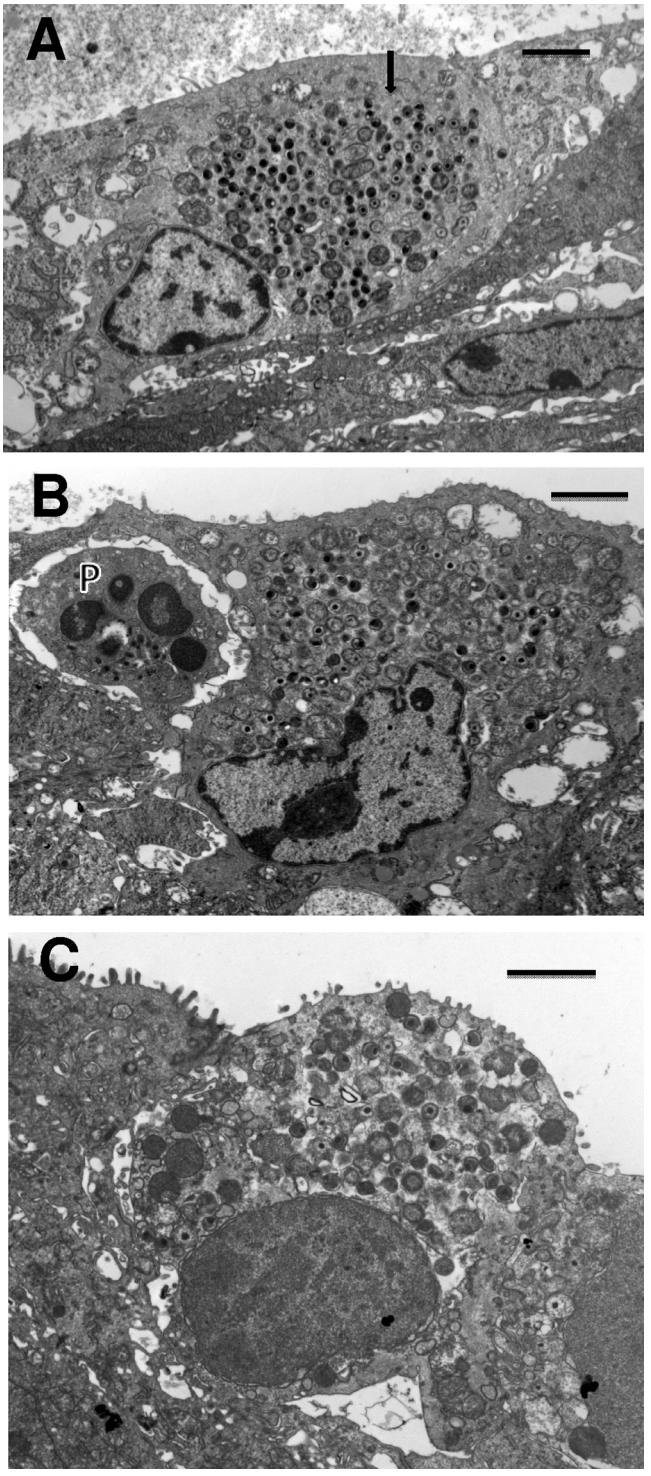

FIG. 5. Termination of the developmental cycle by breakdown of the inclusion membrane. (A) Host epithelial cell with multiple RBs and EBs distributed in the cytoplasm (arrow). The inclusion membrane is no longer obvious. (B) Similar micrographs showing a terminal infected cell with chlamydiae freely distributed in the cytoplasm. A PMN (P) is adjacent to the infected cell. (C) Terminal infected cell with chlamydiae distributed in the cytoplasm. The cell is in the process of being dislodged from the epithelial layer. Scale bars: 2 μm (A and C), 10 μm (B).

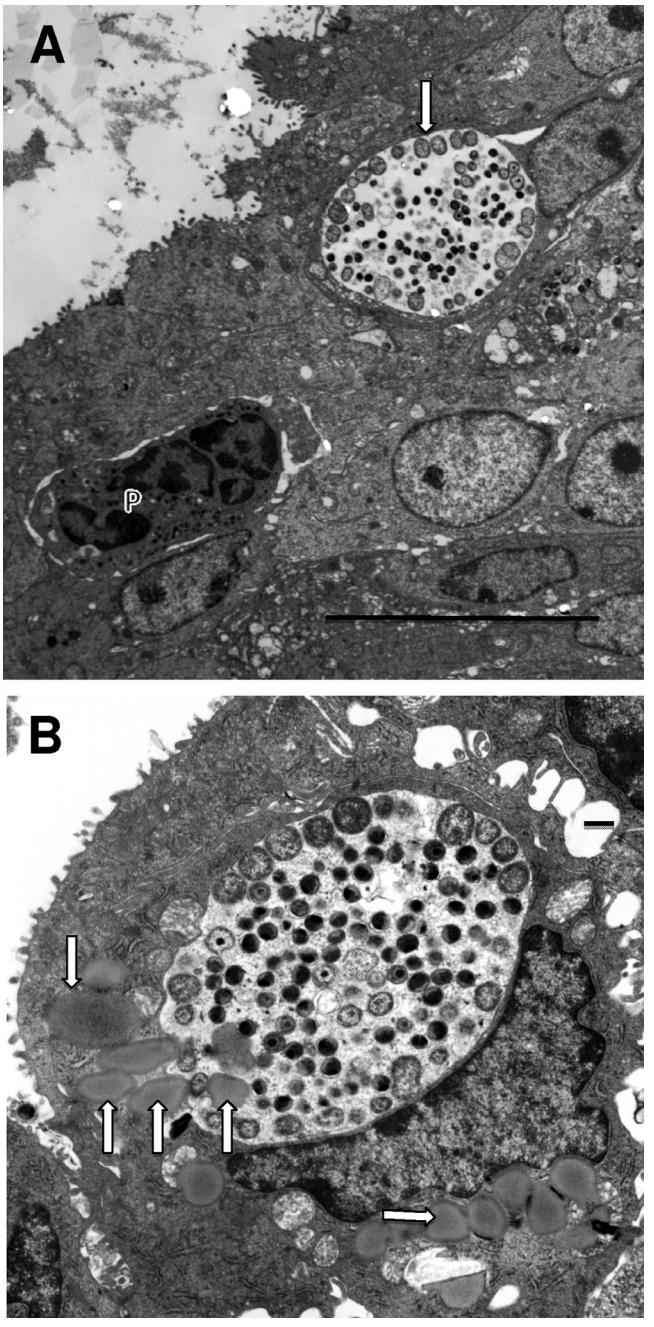

FIG. 6. Inclusions at 42 h after infection. (A) Note that the majority of the RBs in this inclusion (arrow) are along the periphery of the inclusion adjacent to the inclusion membrane while the EBs are in the internal portion. (B) Again, the majority of the RBs are attached to the inclusion membrane. Note the multiple lipid droplets (arrows) in the infected cell. On the left side of the inclusion, lipid droplets are actually entering the inclusion, suggesting an active process of droplet translocation. Scale bars: 10 μm (A), 500 nm (B).

aberrant RBs and normal-sized RBs as well as EBs (Fig. 9B). It was not uncommon to find both inclusions with aberrant RBs and normal inclusions in adjacent cells (Fig. 9A to C). Nevertheless, while the observation of inclusions with aberrant RBs was not uncommon, the majority of inclusions were normal inclusions characteristic of this time in the developmental

TABLE 1. Area of RBs at different times after infection

Hours after infection	Group	Area (μm^2)	Median	No. of RBs measured	Significance (P value)
24		1.09 ± 0.52	0.91	38	
30		0.58 ± 0.28	0.51	52	<0.001[a]
36		0.22 ± 0.12	0.19	94	<0.001[a,b]
36	Membrane attached	0.28 ± 0.14	0.23	20	
36	Membrane not attached	0.20 ± 0.11	0.17	74	<0.003[c]

[a] Compared to the 24-h group by one-way ANOVA.
[b] Compared to the 30-h group by one-way ANOVA.
[c] Compared to the membrane-attached group by one-tailed t test.

cycle. It should be noted that we have refrained from calling the inclusions with aberrant RBs "persistent" inclusions as others do, because we have observed these only within the scope of the first developmental cycle.

DISCUSSION

So much of what we know about the chlamydial developmental cycle is based on studies of the *in vitro* growth of chlamydiae in a variety of cell cultures. While it is easy to characterize morphological and molecular events by observing cultures at defined times after inoculation, and while one may use cultured cells derived from genital tract tissues of humans and animals, the problem, nevertheless, is that one is observing a single cell type in artificial medium in the absence of a host response. Thus, one must always be suspect of the information gained, because the cell culture system is not a true representation of the *in vivo* milieu. The only way to truly understand the interaction of chlamydiae and the host is to evaluate the chlamydial infection in the living animal at the actual site of infection. Such *in vivo* observations using various animal models have given us a strong understanding of the host immune response to infection, but there has been a paucity of information regarding the events in the local cellular milieu, particularly as the events relate to stages in the developmental cycle of chlamydiae. Therefore, in this study, we used a recently developed model of direct intracervical inoculation that produces, at least through the first developmental cycle, a synchronous infection, such that in sampling at various times after inoculation, one finds that the majority of the inclusions are at approximately the same stage (21). This methodology allowed us to characterize the temporal onset of the chemokine and cytokine response in the initial developmental cycle. We now extend this model to sequentially characterize at the ultrastructural level the cellular events associated with the *in vivo* developmental cycle.

In general, the sequence of events in the developmental cycle *in vivo* is the same as that *in vitro*; only the time frame appears to be delayed in comparison to cell culture. While in cell culture, EBs have infected host cells and begun the transition to RBs within a few hours, we still observed single EBs and single RBs 18 h after inoculation (24). *In vitro*, the transition from RB to EB occurred between 12 and 20 h, but we observed this transition between 30 and 36 h *in vivo*. That the cycle would be "delayed" *in vivo* is not unexpected, since even with direct inoculation of organisms at the cervix, there is still a layer of mucus that could impede or at least slow down attachment of EBs to the epithelial cells. Once active infection was noted at 18 h, the remainder of the developmental cycle was consistent with the time frame observed *in vitro*. Our observations of the fusion of multiple early inclusions were also consistent with what has been observed *in vitro*. It was reported that fusion occurred between 10 and 12 h postinfection *in vitro* (7, 13). We noted this event between 24 and 30 h postinfection which, considering an 18 h delay in the initiation of infection *in vivo*, would fit the *in vitro* time frame.

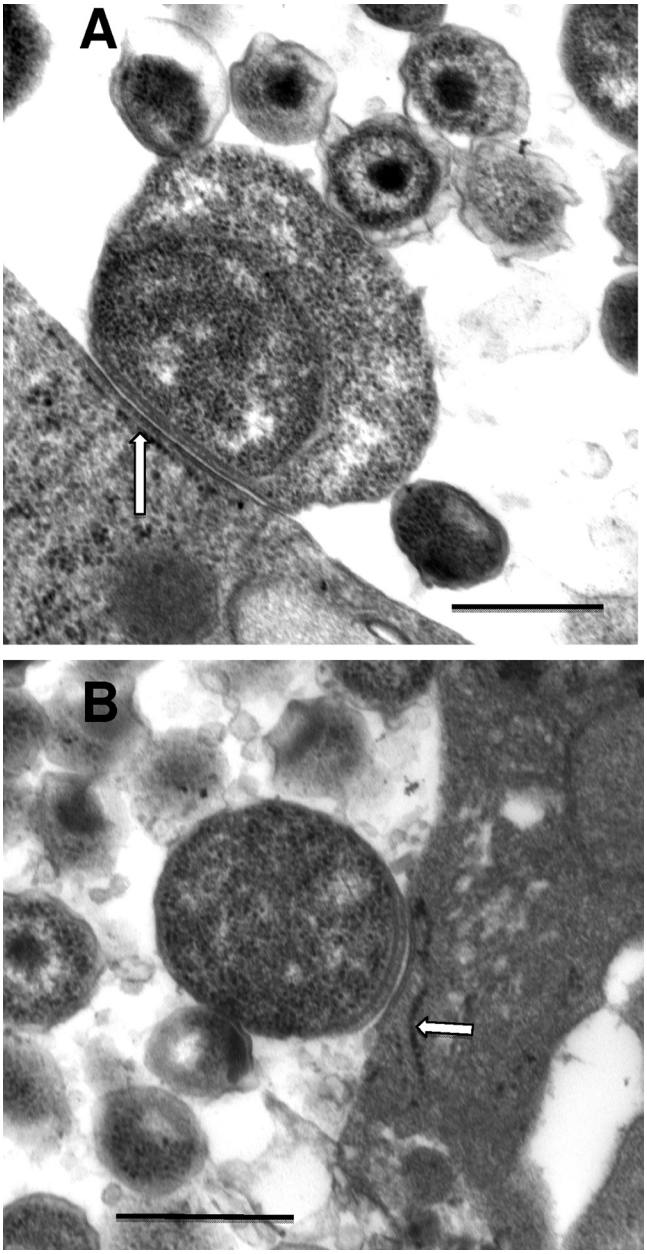

FIG. 7. RBs attached to the inclusion membrane reflecting the contact-dependent hypothesis. (A) Enlarged replicative RB with extensive inclusion membrane contact, likely via the type 3 secretion injectisomes; the contact areas are almost always associated with closely apposed endoplasmic reticulum (arrow), from which the chlamydiae are likely scavenging nutrients. (B) Smaller RB with less extensive area of contact with the inclusion membrane. Scale bars: 500 nm.

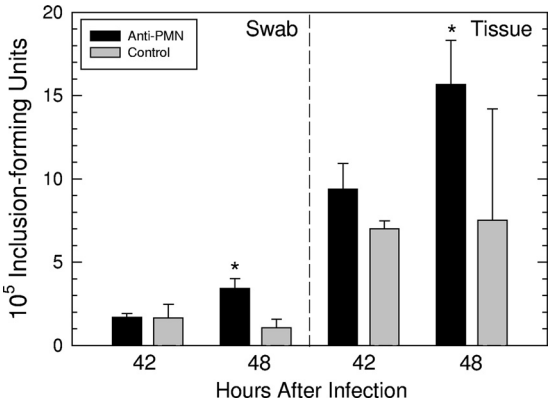

FIG. 8. *In vivo* depletion of PMNs by anti-PMN antibody results in increased number of IFU between 42 and 48 h after infection when quantified from cervicovaginal swabs or directly from cervical tissue. Asterisks indicate that the difference in IFU between 42 and 48 h was significantly different according to a one-tailed *t* test.

Perhaps the most significant observation we have made in this study is the rapid appearance of PMNs in the epithelium and their key role in the terminal stages of the chlamydial developmental cycle. Cell culture studies have suggested a variety of methods by which the cycle may terminate with the ultimate liberation of EBs. These have ranged from spontaneous lysis of the infected cell (15) to extrusion of inclusions (8) to apoptosis of the infected cell (4, 16). Our observations at the ultrastructural level in the mouse cervix suggest three possible mechanisms by which the developmental cycle concludes with the liberation of EBs; in two of these, PMNs play a critical role. In one mechanism, the inclusion develops to a point at which there are primarily EBs and the inclusion membrane breaks down so that chlamydiae are observed directly in the cytoplasm of the cell. Generally, at that time, 42 to 48 h after infection, the cell is not healthy and in some cases is in the process of being dislodged from the epithelium. The likely outcome of a dislodged infected cell is further disintegration of the cell,

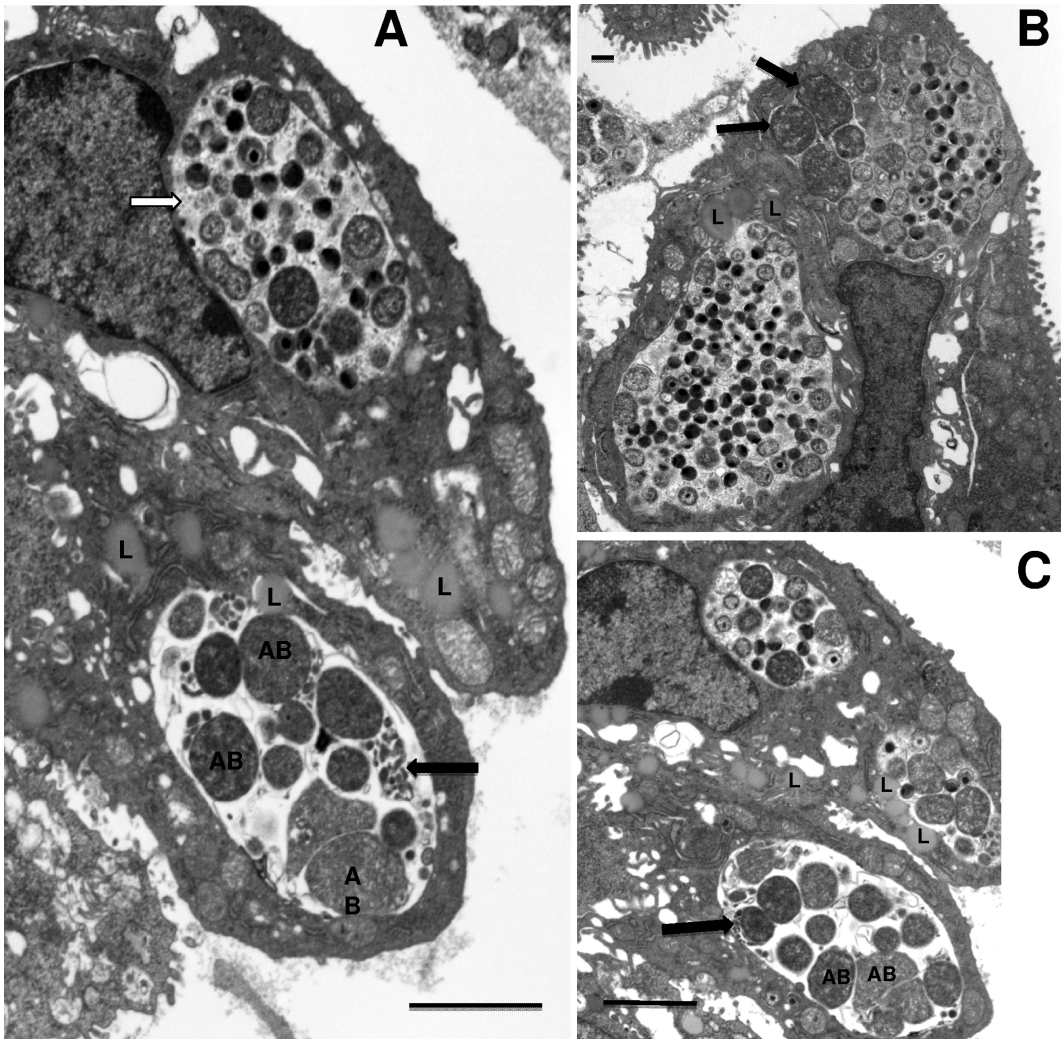

FIG. 9. Inclusions containing aberrant RBs were observed in the cervix of a mouse depleted of PMNs by antibody treatment. (A) Note the large aberrant RBs (AB) as well as packets of miniature RBs (black arrow). Also, this inclusion is devoid of granular material representing glycogen accumulation (white arrow). (B) A large mature inclusion is in the lower left of the photomicrograph, while the upper right inclusion has both aberrant RBs (arrows) and normal size RBs as well as IBs and EBs. (C) Another view showing a normal inclusion (top center) and two inclusions with aberrant RBs (AB), packets of miniature reticulate bodies (arrow), and a lack of glycogen. Scale bars: 2 μm (A and C), 500 nm (B).

liberating the organisms. This mechanism resembles that observed commonly *in vitro*, in which one observes "rounded-up" cells that are losing their attachment to the monolayer. Thus, in this instance, the *in vivo* observations support what has been reported for cell culture. We have seen no *in vivo* evidence for extrusions of inclusions or for morphological evidence of apoptosis of infected cells.

In addition to maturation of the inclusion and ultimate cell lysis, we observed two potential mechanisms by which PMNs participate in the termination of the chlamydial developmental cycle. We previously observed in histopathologic sections that PMNs appear in the submucosa by 12 h after infection and were present in the epithelium by 24 h (21). Electron micrographs taken at 24 h confirmed the presence of PMNs in the epithelium, often in direct contact with infected cells, even cells with only a single visible RB. Beginning at 36 h postinfection, PMNs were appearing to dislodge infected cells from the epithelium. We previously described this phenomenon for conjunctival infections of guinea pigs with *C. caviae*, although at a later time, 4 days after infection (22). Thus, in this exit strategy, infected cells may be "pushed" off the epithelium into the lumen where, ultimately, the cell will die and liberate organisms. Moreover, this may represent a mechanism by which chlamydiae can move to other tissue sites or be available for transmission to new host epithelial cells (22).

We also observed PMNs that have actually entered the infected cell and are in contact with the inclusion. Other views showed PMNs in direct contact with chlamydiae after the disintegration of the inclusion membrane and, in some cases, PMNs within a space containing cell debris and chlamydiae. One cannot state conclusively that this represents a true sequence of events, i.e., invasion of the host cell by the PMN, destruction of the inclusion membrane, and finally, destruction of the host cell liberating chlamydiae; nevertheless, that PMNs can actually enter into an infected cell is indeed a novel observation. It has been previously documented that PMNs can leave capillaries by transcellular migration, i.e., enter endothelial cells through pores at nonjunctional sites and then exit on the basal side of the cell (6). However, to our knowledge, this represents the first observation of a PMN entering a chlamydia-infected cell and directly engaging intracellular chlamydiae; as such, this phenomenon represents a new mechanism by which PMNs may effectively terminate the developmental cycle.

It is not surprising that PMNs should be so intimately associated with infected cells. As we have shown previously, genes for tumor necrosis factor alpha (TNF-α) and certain chemokine receptors are expressed as early as 3 h after infection in this model (21). By 12 h after infection, approximately 41 chemokine receptors, chemokines, and cytokines are expressed, including chemokines for PMNs. Because of the observed contact of PMNs with cells bearing very early inclusions, it is obvious that a very strong chemokine gradient has been generated by the infected cell. It has been previously demonstrated that chlamydial molecules, such as lipopolysaccharides (LPS), may be found on the infected cell surface (9, 23) and bacterial chemotactic molecules, such as *N*-formyl-methionyl-leucyl-phenyalanine, are likely produced by chlamydiae as well. These molecules, which are included among pathogen-associated molecular patterns, could serve as recognition ligands for PMNs.

While the PMNs may actually be "helping" chlamydiae by facilitating their release from infected cells, there is no doubt but that PMNs are also important for the host in controlling the infection until the adaptive response can bring about resolution of infection. We demonstrated that even within the scope of the first developmental cycle, PMNs are important for reducing the level of EBs. There was no significant increase in EBs between 42 and 48 h postinfection in normal animals. However, when PMNs were depleted, a significant increase in the number of IFU was observed, indicating that PMNs are very aggressive in phagocytizing and killing chlamydiae. We routinely observed phagocytized RBs and EBs within PMNs, particularly those in the lumen (data not shown).

Interestingly, when the cervix from a PMN-depleted mouse was observed by TEM, inclusions with aberrant RBs were observed. These inclusions contained not only aberrant RBs but also miniature RBs, and the inclusions were markedly deficient in glycogen, all characteristics of the stress response produced *in vitro* by the administration of IFN-γ or penicillin (1, 2, 14). This is the first report clearly demonstrating aberrant RBs in a natural infection with *C. muridarum*. Phillips and Burillo reported the presence of aberrant RBs, but they were not as clearly defined as in the micrographs from the current study (17). However, they too noted that inclusions may contain aberrant and morphologically normal forms. Recently, Pospischil and colleagues reported the presence of inclusions with aberrant RBs in intestinal infection in swine with *Chlamydia suis* (19). They observed these inclusions within 1 to 2 weeks of oral infection but did not report if they could be observed for chronic infections. In our study, we did observe cells morphologically similar to NK cells in the cervical epithelium, and we have previously demonstrated that NK cells can be found in the cervix as early as 12 to 24 h after genital infection with *C. muridarum* (27). Thus, it is highly likely that the inclusions containing aberrant RBs were the result of IFN-γ in the local microenvironment. It is interesting that we saw them only in an animal deficient in PMNs, but it is likely that the presence of PMNs in normal animals obscured the observation of these inclusions through their microbicidal activity on infected cells and the contained chlamydiae, or there were fewer aberrant forms because of the activity of PMNs. Nevertheless, these data suggest that IFN-γ may affect chlamydiae *in vivo* in a fashion similar to that observed in tissue culture. It still remains to be proven whether chlamydiae in a chronic infection in humans or animal models are present in this form. It is important to note that the majority of inclusions in the tissue where inclusions with aberrant RBs were observed were in fact normal, and some inclusions had aberrant RBs as well as normal RBs and EBs.

We also made observations *in vivo* that confirmed observations from *in vitro* experiments, verifying that these phenomena are not solely *in vitro* artifacts but accurately reflect *in vivo* reality. We routinely observed by TEM, particularly from 24 to 36 h after infection, that the average size of the RBs became smaller with time and that those RBs attached to the inclusion membrane were larger than those that were not attached. This phenomenon was reported by Wilson et al. (28) based on previous ultrastructural observations by Matsumoto (10, 11) of inclusions within cells grown in culture. They presented a mathematical model that supported the contact-dependent hypothesis of chlamydial development that RBs require attach-

ment to the inclusion membrane by the type III secretion injectisomes in order to metabolize and replicate. However, when the RBs have divided to the point at which there is insufficient room to remain attached, forcing detachment from the inclusion membrane and coupled disruption of type III secretion activity, this acts as a signal for the RB to begin the transformation into an EB. When we measured the area of all RBs, whether attached to the inclusion membrane or not, from 24 to 36 h, there was a significant decrease in the area of the RBs as one would expect as the end of the developmental cycle nears. In addition, while quite evident visually, we found that the area of attached RBs was also significantly greater than RBs that had become detached, further supporting *in vivo* the contact-dependent hypothesis that was established through *in vitro* observations.

Finally, it has been recently reported by Cocchiaro et al. (5), using HeLa cells infected with *C. trachomatis* L2, that lipid droplets found in the host cells are translocated into the chlamydial inclusion in an active process mediated by chlamydiae. This was quite novel in that it indicates that chlamydiae are capable of sequestering host cellular organelles for specific purposes. In this study, we were able to visualize lipid droplets adjacent to chlamydial inclusions and actually entering the inclusion. Thus, the translocation of lipid droplets is not restricted to *in vitro* culture but is clearly a mechanism employed by chlamydiae *in situ* in an actual infection model and further demonstrates the utility of this model for confirmation of phenomena observed *in vitro*.

In summary, we have presented for the first time a sequential analysis of the chlamydial developmental cycle at the actual target site of an *in vivo* infection. This model has allowed us to present potential mechanisms by which the developmental cycle terminates and has shown the critical role that PMNs play in the termination of the cycle as well as the early control of the infection. Importantly, this model provides an opportunity to evaluate phenomena previously only described for *in vitro* cell cultures and to determine how predictive these are of the actual *in vivo* reality.

ACKNOWLEDGMENTS

This study was supported by grant AI13446 (P.B.W.) from the NIAID, NIH, the Arkansas Children's Hospital Research Institute (R.G.R.), and the Arkansas Biosciences Institute (R.G.R.).

We thank Patrik Bavoil for critically reading the manuscript.

REFERENCES

1. **Beatty, W. L., G. I. Byrne, and R. P. Morrison.** 1993. Morphologic and antigenic characterization of interferon gamma-mediated persistent *Chlamydia trachomatis* infection *in vitro*. Proc. Natl. Acad. Sci. U. S. A. **90:**3998–4002.
2. **Beatty, W. L., R. P. Morrison, and G. I. Byrne.** 1994. Persistent chlamydiae: from cell culture to a paradigm for chlamydial pathogenesis. Microbiol. Rev. **58:**686–699.
3. **Bedson, S. P., and J. O. W. Bland.** 1932. A morphological study of psittacosis virus, with the description of a developmental cycle. Brit. J. Exp. Pathol. **13:**461–466.
4. **Byrne, G. I., and D. M. Ojcius.** 2004. Chlamydia and apoptosis: life and death decisions of an intracellular pathogen. Nat. Rev. Microbiol. **2:**802–808.
5. **Cocchiaro, J. L., Y. Kumar, E. R. Fischer, T. Hackstadt, and R. H. Valdivia.** 2008. Cytoplasmic lipid droplets are translocated into the lumen of the Chlamydia trachomatis parasitophorous vacuole. Proc. Natl. Acad. Sci. U. S. A. **105:**9379–9384.
6. **Feng, D., J. A. Nagy, K. Pyne, H. F. Dvorak, and A. M. Dvorak.** 1998. Neutrophils emigrate from venules by a transendothelial cell pathway in response to FMLP. J. Exp. Med. **187:**903–915.
7. **Hackstadt, T., M. A. Scidmore-Carlson, E. I. Shaw, and E. R. Fischer.** 1999. The Chlamydia trachomatis IncA protein is required for homotypic vesicle fusion. Cell Microbiol. **1:**119–130.
8. **Hybiske, K., and R. S. Stephens.** 2007. Mechanisms of host cell exit by the intracellular bacterium *Chlamydia*. Proc. Natl. Acad. Sci. U. S. A. **104:**11430–11435.
9. **Karimi, S. T., R. H. Schloemer, and C. E. Wilde.** 1989. Accumulation of chlamydial lipopolysaccharide antigen in the plasma membranes of infected cells. Infect. Immun. **57:**1780–1785.
10. **Matsumoto, A.** 1981. Electron microscopic observations of surface projections and related intracellular structures of Chlamydia organisms. J. Electron Microsc. (Tokyo) **30:**315–320.
11. **Matsumoto, A.** 1981. Isolation and electron microscopic observations of intracytoplasmic inclusions containing *Chlamydia psittaci*. J. Bacteriol. **145:**605–612.
12. **Matsumoto, A.** 1988. Structural characteristics of chlamydial bodies, p. 21–45. *In* A. Barron (ed.), Microbiology of *Chlamydia*. CRC Press, Boca Raton, FL.
13. **Matsumoto, A., H. Bessho, K. Uehira, and T. Suda.** 1991. Morphological studies of the association of mitochondria with chlamydial inclusions and the fusion of chlamydial inclusions. J. Electron Microsc. (Tokyo) **40:**356–363.
14. **Matsumoto, A., and G. P. Manire.** 1970. Electron microscopic observations on the effects of penicillin on the morphology of *Chlamydia psittaci*. J. Bacteriol. **101:**278.
15. **Neeper, I. D., D. L. Patton, and C.-C. Kuo.** 1990. Cinematographic observations of growth cycles of *Chlamydia trachomatis* in primary cultures of human amniotic cells. Infect. Immun. **58:**2042–2047.
16. **Ojcius, D. M., P. Souque, J. L. Perfettini, and A. Dautry-Varsat.** 1998. Apoptosis of epithelial cells and macrophages due to infection with the obligate intracellular pathogen *Chlamydia psittaci*. J. Immunol. **161:**4220–4226.
17. **Phillips, D. M., and C. A. Burillo.** 1998. Ultrastructure of the murine cervix following infection with *Chlamydia trachomatis*. Tissue Cell **30:**446–452.
18. **Phillips, D. M., C. E. Swenson, and J. Schachter.** 1984. Ultrastructure of *Chlamydia trachomatis* infection of the mouse oviduct. J. Ultrastruct. Res. **88:**244–256.
19. **Pospischil, A., N. Borel, E. H. Chowdhury, and F. Guscetti.** 2009. Aberrant chlamydial developmental forms in the gastrointestinal tract of pigs spontaneously and experimentally infected with *Chlamydia suis*. Vet. Microbiol. **135:**147–156.
20. **Ramsey, K. H., L. S. F. Soderberg, and R. G. Rank.** 1988. Resolution of chlamydial genital infection in B-cell-deficient mice and immunity to reinfection. Infect. Immun. **56:**1320–1325.
21. **Rank, R. G., et al.** 2010. Host chemokine and cytokine response in the endocervix within the first developmental cycle of *Chlamydia muridarum*. Infect. Immun. **78:**536–544.
22. **Rank, R. G., J. Whittimore, A. K. Bowlin, S. Dessus-Babus, and P. B. Wyrick.** 2008. Chlamydiae and polymorphonuclear leukocytes: unlikely allies in the spread of chlamydial infection. FEMS Immunol. Med. Microbiol. **54:**104–113.
23. **Richmond, S. J., and P. Stirling.** 1981. Localization of chlamydial group antigen in McCoy cell monolayers infected with *Chlamydia trachomatis* or *Chlamydia psittaci*. Infect. Immun. **34:**561–570.
24. **Shaw, E. I., et al.** 2000. Three temporal classes of gene expression during the *Chlamydia trachomatis* developmental cycle. Mol. Microbiol. **37:**913–925.
25. **Soloff, B. L., R. G. Rank, and A. L. Barron.** 1982. Ultrastructural studies of chlamydial infection in guinea pig urogenital tract. J. Comp. Pathol. **92:**547–558.
26. **Soloff, B. L., R. G. Rank, and A. L. Barron.** 1985. Electron microscopic observations concerning the in vivo uptake and release of the agent of guinea pig inclusion conjunctivitis (*Chlamydia psittaci*) in guinea pig exocervix. J. Comp. Pathol. **95:**335–344.
27. **Tseng, C. K., and R. G. Rank.** 1998. Role of NK cells in the early host response to chlamydial genital infection. Infect. Immun. **66:**5867–5875.
28. **Wilson, D. P., P. Timms, D. L. McElwain, and P. M. Bavoil.** 2006. Type III secretion, contact-dependent model for the intracellular development of chlamydia. Bull. Math. Biol. **68:**161–178.
29. **World Health Organization.** 1975. Isolation of Chlamydia, p. 21–31. *In* Guide to the laboratory diagnosis of trachoma. World Health Organization, Geneva, Switzerland.
30. **Wyrick, P. B., et al.** 1989. Entry of genital *Chlamydia trachomatis* into polarized human epithelial cells. Infect. Immun. **57:**2378–2389.
31. **Wyrick, P. B., et al.** 1994. *Chlamydia trachomatis* antigens on the surface of infected human endometrial epithelial cells. Immunol. Infect. Dis. **4:**131–141.

Editor: B. A. McCormick